

# Results from a High-Sensitivity Search for Cosmic Axions

C. Hagmann, D. Kinion, W. Stoeffl, and K. van Bibber

*Lawrence Livermore National Laboratory*

*7000 East Ave., Livermore, CA 94550*

E. Daw, H. Peng, and L.J Rosenberg

*Department of Physics and Laboratory for Nuclear Science*

*Massachusetts Institute of Technology*

*77 Massachusetts Ave., Cambridge, MA 02139*

J. LaVeigne, P. Sikivie, N.S. Sullivan, and D.B. Tanner

*Department of Physics, University of Florida*

*Gainesville, FL 32611*

F. Nezrick

*Fermi National Accelerator Laboratory*

*Batavia, IL 60510-0500*

Michael S. Turner

*Theoretical Astrophysics, Fermi National Accelerator Laboratory*

*Batavia, IL 60510-0500*

*Departments of Astronomy & Astrophysics and Physics, Enrico Fermi Institute*

*The University of Chicago, Chicago, IL 60637-1433*

D.M. Moltz and J. Powell

*Lawrence Berkeley National Laboratory*

*1 Cyclotron Rd., Berkeley, CA 94720*

N.A. Golubev

*Institute for Nuclear Research of the Russian Academy of Sciences*

*60th October Anniversary Prospekt 7a*

*117 312 Moscow, Russia*

Accepted for Publication in Physical Review Letters

## Abstract

We report the first results of a high-sensitivity ( $\sim 10^{-23}$  W) search for light halo axions through their conversion to microwave photons. At 90% confidence we exclude a KSVZ axion of mass  $2.9 \times 10^{-6}$  eV to  $3.3 \times 10^{-6}$  eV as the dark matter in the halo of our Galaxy.

14.80.Mz, 95.35.+d, 98.35.Gi

The dynamics of galaxies and of clusters of galaxies, as well as their peculiar motions, imply that most of the mass of the Universe is in an unseen form, called ‘dark matter’. The amount of dark matter inferred is at least 20% of the critical density, and likely much more [1]. Because the synthesis of the light elements in the big bang restricts baryons to contribute no more than 10% of the critical density, a large nonbaryonic component is required. The development of structure in the Universe – galaxies, clusters, and superclusters – and the anisotropies of the cosmic background radiation also support this conclusion.

The axion is a well-motivated particle dark matter candidate, arising in models where the strong-CP problem is solved by the Peccei-Quinn mechanism [2]. The axion mass is constrained by laboratory experiments and astrophysical limits to lie between  $10^{-6}$  eV and  $10^{-3}$  eV, with lower masses preferred if axions provide the bulk of the critical density [3].

If the dark matter is ‘cold’ (small velocity dispersion), as is indicated by studies of structure formation, galactic halos are comprised primarily of cold dark matter particles. Because dark matter axions were produced in a coherent process in the early universe, they are cold [4]. Modeling of the Milky Way galaxy indicates a local halo density  $\rho_{halo}$  of  $0.45 \text{ GeV cm}^{-3}$  (about  $7.5 \times 10^{-25} \text{ g cm}^{-3}$ ) [5], that implies an enormous local density  $\mathcal{O}(10^{14} \text{ cm}^{-3})$  of axions if they are the dark matter. The velocity distribution of dark matter particles is expected to be approximately Maxwellian, with a dispersion of  $\langle \beta^2 \rangle^{1/2} \simeq 270 \text{ km/sec}$  [6]. There could also be narrow peaks in the velocity distribution from dark matter particles which have recently fallen into the galaxy and have yet to thermalize [7]. Because of its two-photon coupling,  $\mathcal{L}_{a\gamma\gamma} = -g_{a\gamma\gamma} a \vec{E} \cdot \vec{B}$ , an axion can convert to a single photon in the presence of a magnetic field [8]. Here  $g_{a\gamma\gamma} = g_\gamma \alpha / \pi f_a$ ,  $f_a$  is the axion decay constant, the axion mass  $m_a \simeq 6 \mu\text{eV}$  ( $10^{12} \text{ GeV} / f_a$ ), and  $g_\gamma$  is a model-dependent coefficient of order unity. In two popular models of the axion,  $g_\gamma = -0.97$  (KSVZ) and 0.36 (DFSZ) [2].

In a static magnetic field, the energy of the photon equals that of the converted axion:  $E_\gamma = E_a = m_a + m_a \beta^2 / 2 = m_a (1 + \mathcal{O}(10^{-6}))$ . The conversion process is resonantly enhanced in a high-Q cavity with resonant frequency  $f_0$  tuned to  $E_\gamma$ , with power given by [8]

$$P = \left( \frac{\alpha g_\gamma}{\pi f_a} \right)^2 V B_0^2 \rho_a C \frac{1}{m_a} \text{Min}(Q_L, Q_a) \quad (1)$$

where  $V$  is the volume of the cavity,  $Q_L$  is the loaded quality factor of the cavity,  $B_0$  is the central magnetic field strength,  $\rho_a$  is the local axion density, and  $1/Q_a \sim 10^{-6}$  is the width of the axion energy distribution. The mode-dependent form factor  $C$  is of order unity for the  $\text{TM}_{010}$  mode used in our search and falls off rapidly for higher order modes. For the parameters of this experiment and the KSVZ model,  $P \sim 5 \times 10^{-22}$  W.

Because the axion mass is unknown, the cavity resonant frequency must be tuned. When the  $\text{TM}_{010}$  resonant frequency is close to the axion mass, the conversion of axions to photons produces a narrow peak of fractional width  $\sim 10^{-6}$  in the cavity power spectrum. The noise background is characterized by an effective system temperature  $T_s = T_c + T_a$ , where  $T_c$  is the cavity physical temperature and  $T_a$  is the amplifier noise temperature.

Figure 1 is a schematic diagram of the axion detector, which is located at LLNL [9]. The magnet is a superconducting solenoid of 7.6 T central field. The cylindrical cavity (50 cm i.d., 100 cm long) is constructed of stainless steel plated with copper and subsequently annealed. The temperature of the cavity is  $T_c \sim 1.3$  K. The resonant frequency  $f_0$  of the empty cavity is 460 MHz. The unloaded Q, including losses in the tuning rods, is  $\sim 200,000$ , the limit set by the anomalous skin depth of copper. Two copper tuning rods, each 8 cm in diameter, run the full length of the cavity. The cavity is tuned by moving the rods radially between the wall and center. The cavity is normally evacuated, but can be filled with liquid helium to shift the frequency from the vicinity of mode crossings. There are two coupling ports in the top of the cavity, one weakly coupled and the other of variable coupling strength. Power is extracted from the variable port through a  $50 \Omega$  transmission line, which is 50 cm long, to a directional coupler and amplifier chain. The weakly coupled port and the 30dB directional coupler provide for transmission and reflection measurements of cavity parameters. The coupling at the variable port is adjusted to near critical.

The first- and second-stage amplifiers are balanced GaAs HEMT devices built by the National Radio Astronomy Observatory (NRAO). They are cooled to the cavity temperature

and are characterized by noise temperature  $T_a \sim 4.5\text{K}$ , power gain of  $G \sim 17\text{dB}$ , and power reflection coefficient from the input of  $\sim 30\text{dB}$  [10]. The amplifier noise temperature is measured by varying the physical temperature of the cavity and extrapolating the amplifier output to zero physical temperature.

After 35dB of further amplification at room temperature, the signal is down-converted to 10.7 MHz by an image-rejection mixer. An 8-pole crystal filter sets the 30 kHz measurement bandwidth and prevents image power from entering the second mixing stage. The signal is then down-converted a second time, in effect shifting the cavity resonant frequency to 35 kHz.

A commercial FFT spectrum analyzer then generates the ‘medium-resolution’ power spectrum. During each 80-second run, 10,000 sub-spectra are measured and averaged, resulting in a 400 point, 125 Hz/point power spectrum. This is well-matched to a search for the Maxwellian component of the halo, which should be about 6 channels wide.

The analog output is also applied to a 6-pole filter followed by a third mixing stage centering the cavity resonant frequency at 5 kHz. This signal is processed by a commercial ADC/DSP PC board, yielding the ‘high-resolution’ power spectrum. There is no averaging, but rather one 250,000 point, 0.02 Hz/point power spectrum is generated. This is well matched to a search for fine structure having fractional width  $\sim \mathcal{O}(10^{-11})$  or less in the power spectrum. If any appreciable fraction of the axions are in a narrow-velocity line, it would be detected with high signal-to-noise ratio. A cesium clock serves as the frequency reference for both receivers.

After each 80-second run, the cavity frequency  $f_0$  is tuned upwards by 2 kHz, the loaded cavity quality factor  $Q_L$  is measured, and another run initiated. The dead-time associated with tuning and measuring cavity parameters is about 4 seconds per run. The form factor  $C$  is calculated by a computer simulation of the cavity at each frequency. Each frequency range is swept out, then the procedure is repeated at least twice more. Regions in frequency where TE or TEM modes cross the TM<sub>010</sub> mode are examined by filling the cavity with liquid helium, thus shifting the mode-crossing frequency down by 3%. The overall live-

time of the experiment has been well over 90% since the beginning of data-taking. Of the approximately  $4.2 \times 10^5$  spectra recorded for this analysis, 6058 were eliminated due to anomalously large cavity frequency shifts or pressure jumps, typically related to cryogen fills or other disturbances.

During off-line data processing, the middle 200 frequency bins of each 400 point spectrum are divided by the 8-pole crystal filter response. The resulting power spectrum varies slowly with frequency by  $\sim 1\text{dB}$  across the spectrum due to noise from sources in the amplifier propagating backwards along the transmission line and reflecting from the cavity coupling. To obtain a flat, corrected power spectrum, we remove this slow variation using a 5-parameter equivalent circuit model.

Because the typical 2 kHz tuning step is smaller than the 30 kHz crystal filter bandwidth, and because three or more sweeps are made over the whole frequency range, each 125 Hz bin appears in at least 45 spectra. These spectra are linearly combined with a weighting that accounts for the  $B_0$ ,  $T_s$ ,  $C$ ,  $Q$ ,  $f - f_0$  appropriate for each. The result is a single spectrum of nearly  $10^6$  points between 701-800 MHz. Figure 2 shows (a) the expected signal from KSVZ axions, (b) the noise background were the axion signal distributed over 6 channels, and (c) the noise background were the axion signal confined to 1 channel. Figure 3 shows the deviation of the single channel power from the thermal mean for all the data taken. The distribution is consistent with thermal (Gaussian) noise out to  $5\sigma$ . This is an important validation of our understanding of the experiment.

Candidates for further examination are those single 125 Hz channels with a  $3.3\sigma$  power excess (538 candidates), or the sum of any 6 adjacent 125 Hz channels with a  $2.25\sqrt{6}\sigma$  power excess (6535 candidates). These candidates were then rescanned to the same power sensitivity as the first spectrum. Of the 6-channel (1-channel) candidates, 23 (6) persisted, *i.e.*, appeared independently in the rescan. Of those, 8 (4) were at the same frequency as known external RF sources. The remainder developed power in the tails of the cavity Lorentzian instead of near the peak as would the axion. This behavior is expected for external interference introduced through the calibration ports and reflecting off the cavity

input back into the amplifier. The few persistent candidates were rescanned after terminating calibration lines leading into the cavity; no candidates survived all scans.

Figure 4 shows the axion couplings and masses excluded at the 90% confidence level by this analysis for axions with the expected Maxwellian velocity distribution. At 95% (68%) confidence level, the value of  $g_{a\gamma\gamma}^2/m_a^2$  excluded is approximately  $1.6(1.0) \times 10^{-19} \text{ GeV}^{-2}/\text{eV}^2$ . Also shown are KSVZ and DFSZ model predictions. Indicated on the inset are the regions excluded by earlier microwave cavity experiments [11,12]. The present experiment is more than two orders-of-magnitude more sensitive, and is the first to exclude a well-developed axion model (KSVZ) at a realistic density over any mass range. The significance of this result, however, is not just the exclusion of a given axion model over a narrow mass range at the most probable local cold dark matter density (within the full-width at half-maximum likelihood range of  $4.5\text{--}12 \times 10^{-25} \text{ g cm}^{-3}$  [5]). Equally important, the sensitivity of the microwave cavity scheme has been brought into the region of interest, *i.e.*, where the axion might plausibly be discovered.

The high-resolution channel is analyzed similarly. The power spectra are binned on-line at resolutions 0.02 Hz, 0.16 Hz and 1.3 Hz, for which candidates were defined as those peaks with more than  $15\sigma$ ,  $8\sigma$  and  $5\sigma$  excess power respectively. After rescanning candidate peaks and eliminating external noise peaks, no candidates remained. This procedure resulted in upper power limits near  $3.3 \times 10^{-23} \text{ W}$  (0.02 Hz/channel),  $5.0 \times 10^{-23} \text{ W}$  (0.16 Hz/channel) and  $8.8 \times 10^{-23} \text{ W}$  (1.3 Hz/channel). We further searched for coincidences between medium- and high-resolution candidates, and after excluding obvious external RF sources, found none.

In conclusion, for the first time sufficient sensitivity has been achieved to detect KSVZ axions if they comprise the dark matter of our own galactic halo. Based upon our first results, we exclude at 90% confidence a KSVZ axion of mass between 2.9 and  $3.3 \mu\text{eV}$ , assuming halo axions have a Maxwellian velocity distribution. If a significant fraction of halo axions are distributed in a few narrow peaks, weaker axion two-photon couplings are excluded. Promising developments in amplifier and magnet technologies may soon extend the sensitivity of the experiment by more than an order of magnitude, permitting a search

for axions that couple more weakly (*e.g.*, DFSZ) at lower halo densities.

The authors thank R. Bradley of NRAO for sharing his amplifier expertise. This research is supported by the U.S. Department of Energy under contracts W-7405-ENG-048, DE-AC03-76SF00098, DE-AC02-76CH03000, DE-FC02-94ER40818, DE-FG02-97ER41029 and DE-FG02-90ER40560 and the National Science Foundation grant number PHY-9501959.

## REFERENCES

- [1] See *e.g.*, A. Dekel, D. Burstein, and S.D.M. White, in “Critical Dialogs in Cosmology”, ed. N. Turok, World Scientific, Singapore (1997); or, J. Willick, M.A. Strauss, A. Dekel, and T. Kolatt, *Astrophys. J.* **46**, 629 (1997).
- [2] See *e.g.*, J.E. Kim, *Phys. Reports.* **150**, 1 (1987); H.-Y. Cheng, *ibid.*, **158**, 1 (1988).
- [3] See *e.g.*, M.S. Turner, *Phys. Reports.* **197**, 67 (1990).
- [4] J. Preskill, M. Wise, and F. Wilczek, *Phys. Lett. B.* **120**, 127 (1983); L. Abbott and P. Sikivie, *ibid.*, 133; M. Dine and W. Fischler, *ibid.*, 137.
- [5] E.I. Gates, G. Gyuk and M.S. Turner, *Astrophys. J.* **449**, 123 (1995).
- [6] M.S. Turner, *Phys. Rev. D.* **42**, 3572 (1990).
- [7] P. Sikivie, I.I. Tkachev, Y. Wang, *Phys. Rev. Lett.* **75**, 2911 (1995).
- [8] P. Sikivie, *Phys. Rev. Lett.* **51**, 1415 (1983); L. Krauss *et al.*, *ibid.*, **55**, 1797 (1985); P. Sikivie, *Phys. Rev. D.* **32**, 2988 (1985).
- [9] More details may be found in C. Hagmann *et al.*, *Nucl. Phys. B.* **51**, 209 (1996).
- [10] E. Daw and R.F. Bradley, *J. Appl. Phys.* **82**, 1925 (1997).
- [11] S. DePanfilis *et al.*, *Phys. Rev. Lett.* **59**, 839 (1987); W.U. Wuensch *et al.*, *Phys. Rev. D.* **40**, 3153 (1989). We changed these limits to 90% confidence.
- [12] C. Hagmann *et al.*, *Phys. Rev. D.* **42**, 1297 (1990).

## FIGURES

FIG. 1. Schematic diagram of the axion detector.

FIG. 2. (a) The expected signal from KSVZ axions. (b) The noise background for an axion signal distributed over 6 channels. (c) The noise background for an axion signal confined to 1 channel.

FIG. 3. The distribution of the deviation of single channel noise power from the thermal mean (in units of standard deviation  $\sigma$ ), in each  $0.1 \sigma$  interval, for all the data taken. The curve shows the theoretical expectation (thermal Gaussian noise treated as input to the analysis chain). The slight deviation from Gaussian shape is introduced by the filter response.

FIG. 4. Axion couplings and masses excluded at 90% confidence by this experiment. Also shown are KSVZ and DFSZ model predictions. Indicated on the inset are the regions excluded by earlier microwave cavity experiments; RBF indicates Rochester-BNL-FNAL [11], UF indicates University of Florida [12]. All results are scaled to  $\rho_a = \rho_{halo}$ .

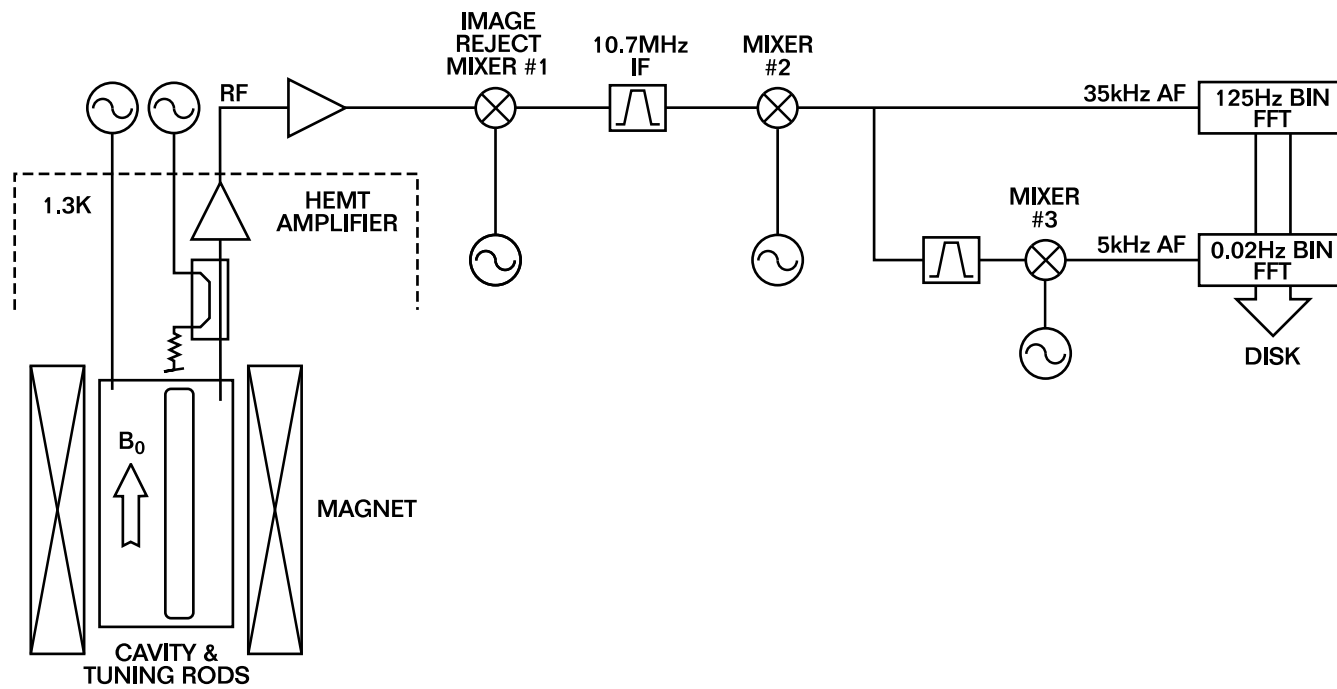


Fig.1

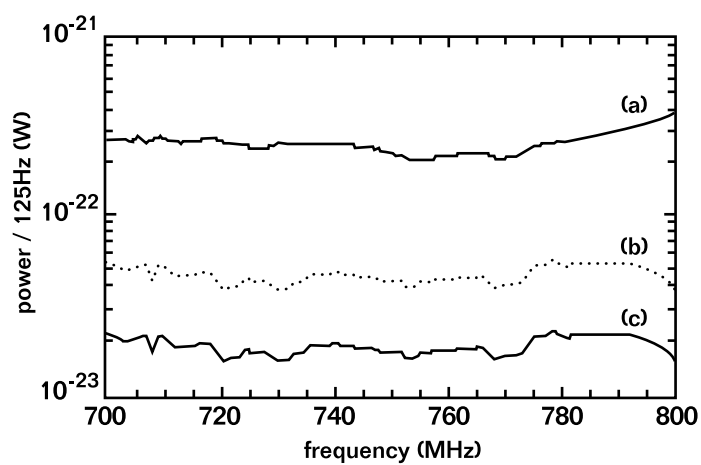


Fig. 2

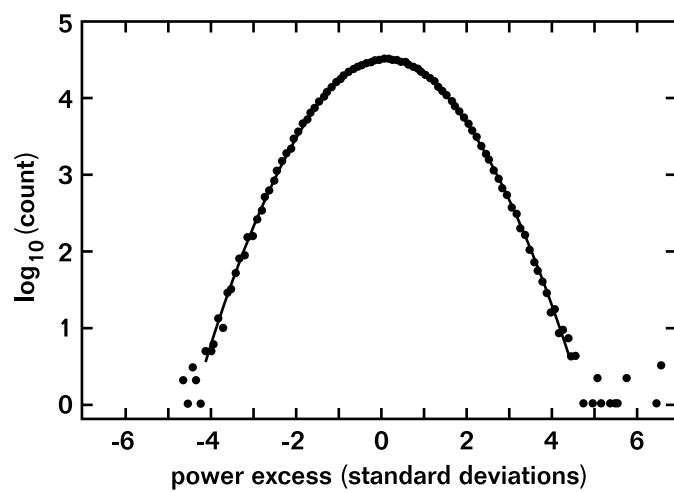


Fig. 3

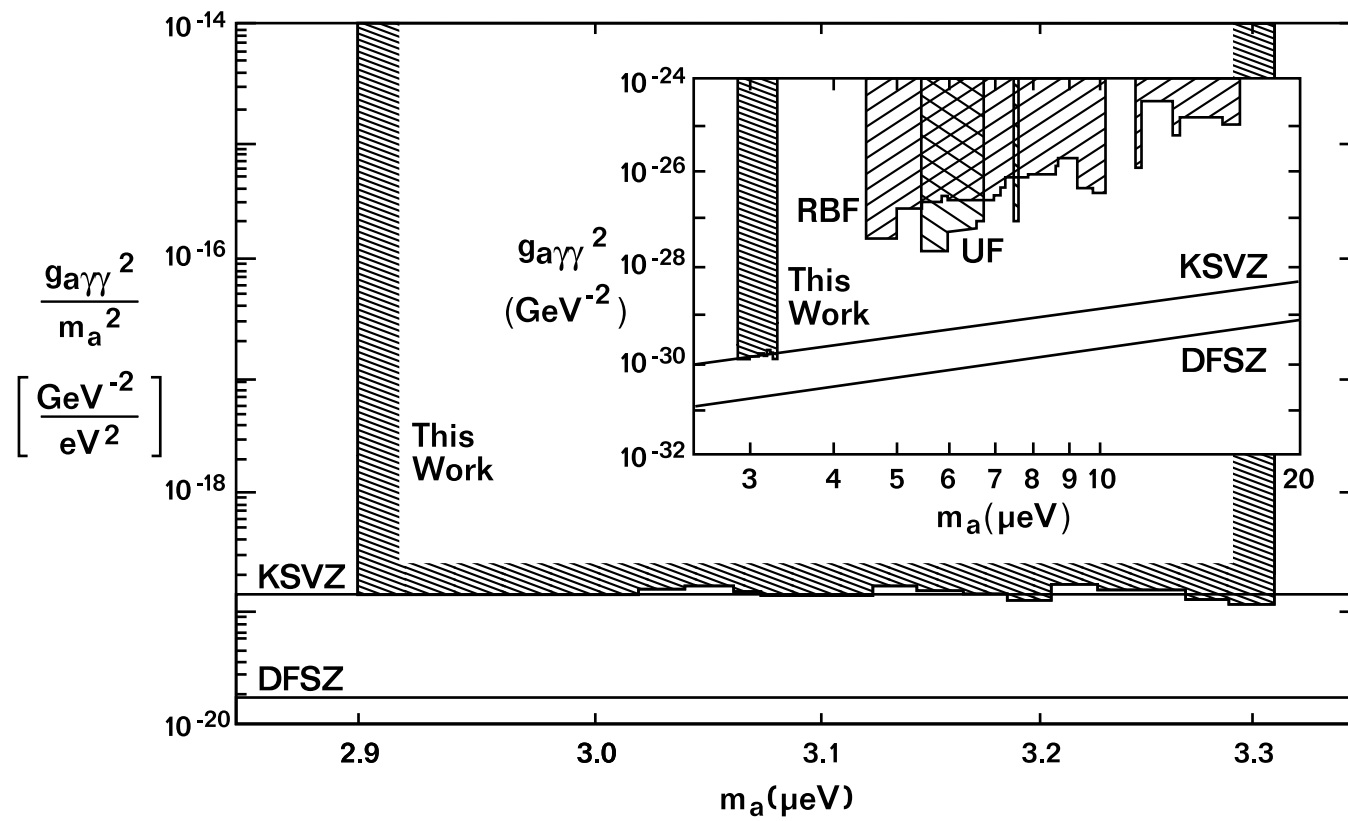


Fig. 4